JOURNAL OF BACTERIOLOGY, May 2006, p. 3442–3448 Vol. 188, No. 10
0021-9193/06/$08.00+0 doi:10.1128/JB.188.10.3442–3448.2006

Diffusion of Green Fluorescent Protein in Three Cell Environments in *Escherichia Coli*

Conrad W. Mullineaux,[1]* Anja Nenninger,[2] Nicola Ray,[2] and Colin Robinson[2]

School of Biological and Chemical Sciences, Queen Mary, University of London, Mile End Road, London E1 4NS, United Kingdom,[1] and Department of Biological Sciences, University of Warwick, Coventry CV4 7AL, United Kingdom[2]

Received 25 November 2005/Accepted 1 March 2006

Surprisingly little is known about the physical environment inside a prokaryotic cell. Knowledge of the rates at which proteins and other cell components can diffuse is crucial for the understanding of a cell as a physical system. There have been numerous measurements of diffusion coefficients in eukaryotic cells by using fluorescence recovery after photobleaching (FRAP) and related techniques. Much less information is available about diffusion coefficients in prokaryotic cells, which differ from eukaryotic cells in a number of significant respects. We have used FRAP to observe the diffusion of green fluorescent protein (GFP) in cells of *Escherichia coli* elongated by growth in the presence of cephalexin. GFP was expressed in the cytoplasm, exported into the periplasm using the twin-arginine translocation (Tat) system, or fused to an integral plasma membrane protein (TatA). We show that TatA-GFP diffuses in the plasma membrane with a diffusion coefficient comparable to that of a typical eukaryotic membrane protein. A previous report showed a very low rate of protein diffusion in the *E. coli* periplasm. However, we measured a GFP diffusion coefficient only slightly smaller in the periplasm than that in the cytoplasm, showing that both cell compartments are relatively fluid environments.

The diffusion of cell components is crucial to the function of all living cells. Diffusion may be particularly important in prokaryotes, where systems of active transport appear to be much less developed than those in eukaryotes. We do not know enough about intracellular environments to be able to predict diffusion coefficients with any confidence. For example, macromolecular crowding, the presence of large, relatively immobile protein structures, and interactions with other molecules will have complex effects on diffusion (7). Therefore it is essential to measure diffusion coefficients experimentally.

Fluorescence recovery after photobleaching (FRAP) provides a simple technique for measuring the diffusion of fluorescent molecules in vivo. Measurements can be carried out using a laser scanning confocal microscope (12, 20); the confocal laser spot is used to bleach out fluorescence in a small region of the cell and subsequently to image the cell. Movement of the fluorophore does not change the total fluorescence from the sample, but it does lead to redistribution of the fluorescence. In the case of random diffusion, the bleach is expected to become broader and shallower with time (11, 14). Depending on the geometry of the measurement, quantitative estimates of diffusion coefficients can often be obtained. As an optical technique, FRAP has limited spatial resolution. It is therefore usually applied to eukaryotic cells, and there have been relatively few instances of the use of FRAP in prokaryotes, where the typically smaller cell sizes can be problematic. However, several groups have shown that quantitative FRAP is possible in elongated bacterial cells (4, 8, 14, 21). An excellent model system is *Escherichia coli* grown in the presence of cephalexin, which inhibits cell division, causing the production of greatly elongated cells (4, 8, 19). Typically, a line is bleached across the short axis of the cell, and diffusion is observed in one dimension along the long axis of the cell (8). Such methods have been used to observe the diffusion of green fluorescent protein (GFP) in the cytoplasm of *E. coli* (8), the diffusion of proteins chemically labeled with fluorophores in the periplasm of *E. coli* (4), and the diffusion of thylakoid membrane components in cyanobacteria (14, 15, 21).

Diffusion coefficients in prokaryotes may differ radically from those in eukaryotes for several reasons. Prokaryotic membranes typically have a rather different lipid composition (16) which may strongly influence the diffusion of membrane proteins. In eukaryotes, the cortical cytoskeleton greatly influences the mobility of many membrane proteins (17, 26). The prokaryotic cytoskeleton is rather different (13); in the cytoplasm, the absence of an extensive cytoskeleton may have a profound effect (7). The periplasmic space is unique to gram-negative bacteria, and its physical properties are largely unknown (4).

Here we report FRAP measurements of GFP diffusion in *E. coli* cells elongated with cephalexin. We used a previously described construct (23) which fuses GFP to the twin-arginine, N-terminal signal peptide of trimethylamine oxide reductase (TorA) with 39 amino acids. The TorA-GFP construct was expressed in a wild-type background, where it is exported to the periplasm via the twin-arginine translocation (Tat) system (23). For comparison, the same construct was expressed in a Δ*tatABCDE* background, where the GFP remains in the cytoplasm (23). Finally, a fusion with the *tat*A gene was used to tag the C terminus of an *E. coli* plasma membrane protein as previously described (19). We report diffusion coefficients for GFP in the three environments.

* Corresponding author. Mailing address: School of Biological and Chemical Sciences, Queen Mary, University of London, Mile End Road, London E1 4NS, United Kingdom. Phone: 44 20 7882 7008. Fax: 44 20 8983 0973. E-mail: c.mullineaux@qmul.ac.uk.

MATERIALS AND METHODS

***E. coli* strains.** The strains of *E. coli* used were all derivatives of the parental strain MC4100, which was selected for arabinose resistance (MC4100AR) (2). The GFP gene was GFPmut3* (6). GFP constructs were expressed using the arabinose-inducible pBAD24 vector (10). The TatA-GFP construct is described in reference 19, and the TorA-GFP construct is described in reference 23. TorA-GFP was expressed in either the wild-type background (MC4100AR) or the Δ*tatABCDE* (24). TatA-GFP was expressed in Δ*tatABCDE* (19).

Growth of cells. *E. coli* strains were grown at 37°C in Luria-Bertani (LB) medium supplemented with ampicillin (50 μg/ml) (2). Prior to measurements, L-arabinose was added to 200 μM and cephalexin was added to 30 μg/ml. Cells were grown for a further 2 to 3 h, harvested by centrifugation, and washed and resuspended in LB medium containing cephalexin but no arabinose. Cells were grown in liquid culture for a further 1 to 2 h. They were then diluted by a factor of approximately 10 in fresh LB with cephalexin and spotted onto LB agar plates. The drops of culture were allowed to dry down onto the plates.

Sample preparation for confocal imaging and FRAP. Small blocks of agar with cells adsorbed to the surface were excised and placed in a laboratory-built microscope sample holder with a glass coverslip gently pressed onto the agar surface (14, 19). Samples were maintained at 37°C by connecting a circulating water bath to the water-jacketed sample holder.

Confocal fluorescence imaging. Images were recorded with a Nikon PCM2000 laser scanning confocal microscope equipped with a 100-mW argon laser (19). The 488-nm laser line was selected with a band-pass interference filter. The sample was visualized with a 60× oil-immersion objective lens (numerical aperture, 1.4) with a 20-μm confocal pinhole. GFP fluorescence was selected with a 505-nm dichroic mirror and an interference band-pass filter transmitting light from about 500 to 527 nm. Images were recorded by scanning the laser over a field of view that was typically 30.8 by 30.8 μm. Images were 512 by 512 pixels, with a scan speed of 3 μs per pixel. Images were averaged from 10 successive scans. The *xy* resolution of the microscope was approximately 250 nm. The *z* resolution was measured by imaging a single bilayer of phosphatidylcholine stained with BODIPY FL-C_{12}, a green lipophilic fluorophore (22). The resolution was dependent on the confocal pinhole used; with the 20-μm confocal pinhole, it was about 0.75 μm (half-width at half-maximum).

FRAP measurements. The conditions described above were adapted as follows: for TatA-GFP, a 50-μm confocal pinhole was used. The laser was run at 100 mW, with the intensity reduced by a factor of 32 with neutral-density filters. Elongated cells aligned in the *y* direction were selected. For photobleaching, the laser intensity was increased by a factor of 32 by withdrawing the neutral-density filters and the laser spot was scanned for 2 to 3 s in the *x* direction. The filters were then replaced, and *xy* image scans were recorded at 4-s intervals (19). For TorA-GFP, the confocal pinhole was opened. Image pixel sizes were reduced to 160 by 160 pixels, with a scan speed of 9.6 μs per pixel. The bleach time was reduced to approximately 0.5 s and postbleach images were recorded at 1-s intervals.

FRAP data analysis. One-dimensional fluorescence profiles were extracted from images as previously described, summing data widthways across the cell (14, 15, 21). Postbleach fluorescence profiles were subtracted from the prebleach profile, and the difference profiles were fitted to a Gaussian curve. Diffusion coefficients were obtained from plots of bleach depth versus time, according the one-dimensional diffusion equation $C = C_0 R_0 (R_0^2 + 8Dt)^{-0.5}$, where t is time, C is the depth of the bleach (C_0 at $t = 0$), R_0 is the initial half-width ($1/e^2$) of the bleach, and D is the lateral diffusion coefficient (14).

The radius of the bleach was measured from the bleaching profile extracted from the first postbleach image (14). Data extraction from images was with Optimas 5.2, and curve fitting was with SigmaPlot. Presented diffusion coefficients are means obtained from measurements of at least six cells with standard deviations.

Cell fractionation and immunoblotting. Cell fractionation and immunoblotting were performed as described previously (23) except that cells were grown in the presence of cephalexin as described above.

RESULTS

Diffusion of TatA-GFP in the plasma membrane. It was previously shown that TatA-GFP is localized in the *E. coli* plasma membrane, where two populations can be distinguished: on average about 75% of TatA-GFP is evenly dispersed in the membrane, whereas about 25% is in highly localized aggregates (19). The TatA-GFP fusion protein is susceptible to proteolytic clipping at the C terminus, but there is no indication that the intact GFP domain can be excised. Thus, we can be confident that all the GFP fluorescence seen in the transformant originates from the TatA-GFP fusion (19). We used qualitative FRAP to show that dispersed material diffuses freely, whereas the aggregated protein is immobile, at least on short time scales, and does not readily exchange with the dispersed material (19).

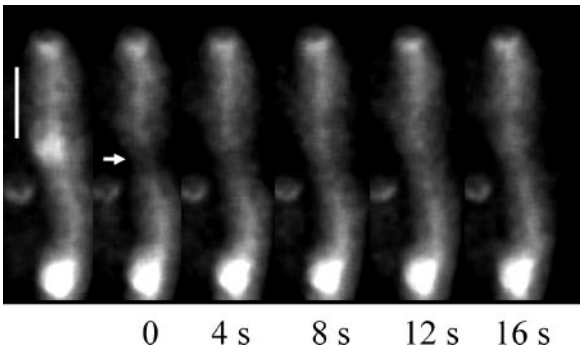

FIG. 1. FRAP image sequence for an elongated *E. coli* cell expressing TatA-GFP localized in the plasma membrane. The far left image is prior to the bleach. The next image is after bleach, and subsequent time in seconds is indicated. The center of the bleach is indicated by the arrow, whose thickness corresponds to the approximate beam width. Scale bar, 5 microns.

To obtain a diffusion coefficient for the dispersed TatA-GFP, we grew cells in the presence of cephalexin in order to generate greatly elongated cells, which are much better for FRAP measurements (4, 8). Cells were laid down on an agar surface under a coverslip and maintained at 37°C as described in Materials and Methods. Under these conditions, we could observe considerable elongation of cells on a time scale of 1 to 2 h, indicating that the cells were healthy and actively growing (not shown). We selected elongated cells with long stretches of dispersed material uninterrupted by aggregates. Figure 1 shows a typical FRAP image sequence for such a cell. Images recorded with the same settings for cells which had not been treated with arabinose to induce TatA-GFP expression showed no significant fluorescence (not shown). Thus, we can be confident that we are monitoring the fluorescence from TatA-GFP rather than that from other, autofluorescent, cell components. When fluorescence was bleached from an entire small cell aligned in the *x* direction, there was no detectable recovery on the 30-s time scale of the measurement (not shown). Thus, the fluorescence recovery we see arises entirely from diffusion rather than from delayed emission or other photochemical phenomena.

Data from FRAP image sequences from TatA-GFP cells were analyzed as described in Materials and Methods. Figure 2 shows an example of extracted one-dimensional fluorescence difference profiles for one cell and estimation of the diffusion coefficient from the time dependence of the depth of the bleach. Note that the bleach becomes both shallower and broader with time, as is characteristic for random diffusion (14). We found that the diffusion coefficient was rather consistent from cell to cell: on average it was 0.13 ± 0.03 (standard deviation), $\mu m^2\ s^{-1}$ ($n = 8$). There was no indication of an immobile population of the dispersed TatA-GFP.

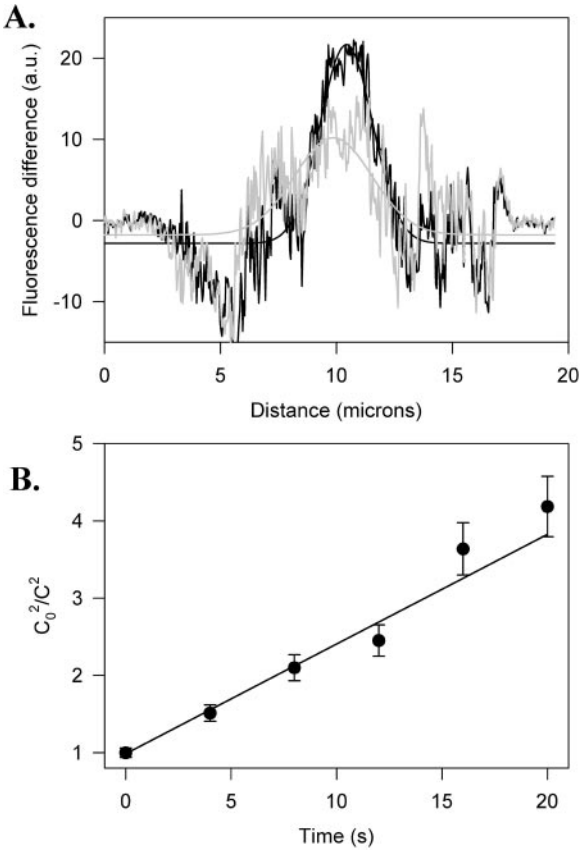

FIG. 2. Data analysis from a FRAP image sequence for an elongated *E. coli* cell with TatA-GFP in the plasma membrane. (A) One-dimensional fluorescence profiles from the first postbleach image (black) and 20 s later (gray). Raw data and fitted Gaussian curves are shown. The *x* axis shows distance along the long axis of the cell, and the *y* axis shows fluorescence difference obtained by subtracting the postbleach fluorescence profiles from the prebleach profile. a.u., arbitrary units. (B) Plot of C_0^2/C^2 versus time, where C is the bleach depth (C_0 in the first postbleach image). The gradient of the line is $8D/R_0^2$, where R_0 is the half-width ($1/e^2$) of the bleach in the first postbleach image (14). Error bars indicate standard deviations.

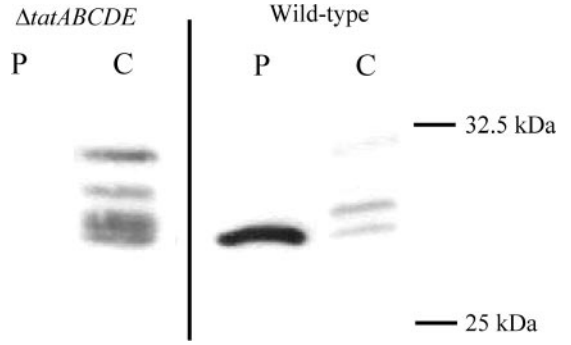

FIG. 4. Immunoblots of *E. coli* cells expressing the TorA-GFP fusion. Cells were grown under the same conditions as for the FRAP measurements, and periplasmic (P) and cytoplasmic (C) fractions were isolated. Fractions were loaded on the basis of the contents of equal numbers of cells. Immunoblotting was performed with an anti-GFP antibody. The distribution of TorA-GFP in the wild-type (MC4100) and Δ*tatABCDE* backgrounds was compared.

Diffusion of TorA-GFP in the cytoplasm. When the TorA-GFP construct is expressed in the wild-type background, it is efficiently exported to the periplasm, accompanied by proteolytic removal of the 39-amino-acid TorA signal peptide (1, 23). To obtain diffusion coefficients for GFP in the cytoplasm and in the periplasm, we expressed the same TorA-GFP construct either in the wild-type background or in a background in which the Tat translocation system is disabled (Δ*tatABCDE*) (24). As previously reported (23), we found that TorA-GFP was localized in the cytoplasm under these conditions (Fig. 3B). There is no significant association between the TorA-GFP and the plasma membrane under these conditions (23). Immunoblots for cytoplasmic and periplasmic fractions from cells grown with cephalexin under the same conditions as those used for the FRAP measurements confirm the cytoplasmic location of GFP in the Δ*tatABCDE* background (Fig. 4). GFP appears in the wild-type background in the periplasm at 27 kDa (Fig. 4), corresponding to the size of a GFP molecule with the TorA signal sequence removed. GFP bands appear in the cytoplasm at sizes ranging from 27 to 30 kDa, presumably due to partial

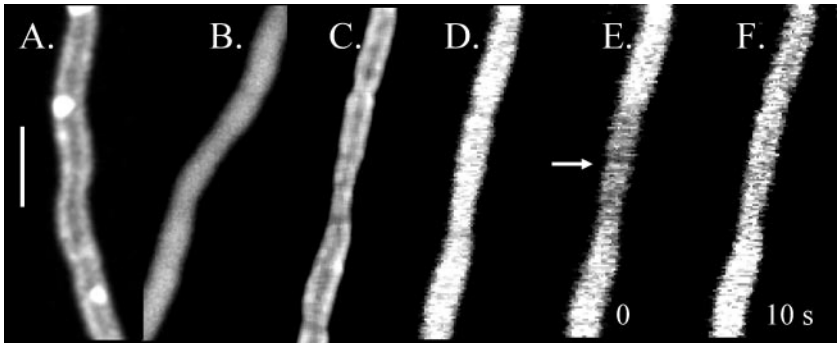

FIG. 3. GFP distributions from fluorescence micrographs of *E. coli* cells elongated by growth in the presence of cephalexin. (A) High-resolution image of a cell expressing TatA-GFP localized in the plasma membrane. (B) High-resolution image of a cell with TorA-GFP in the cytoplasm. (C) High-resolution image of a cell with TorA-GFP exported to the periplasm. (D) Low-resolution image of the same cell as in panel C. This is the prebleach image from a FRAP image sequence. (E) Postbleach image of the same cell as in panels C and D. The site of the bleach is indicated by an arrow, whose thickness corresponds to the approximate beam width. (F) Image of the same cell as in panels C through E at the end of a FRAP image sequence (after 10 s). Scale bar, 5 microns.

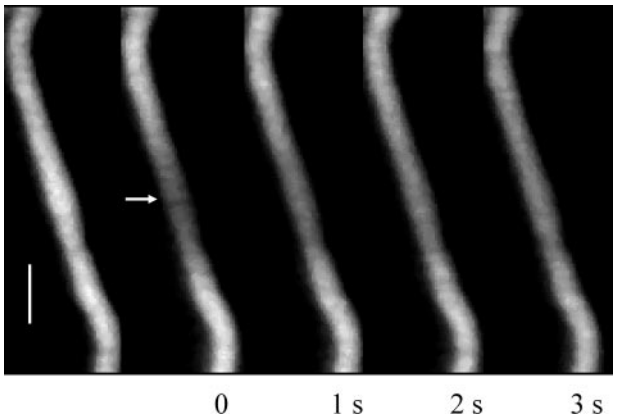

FIG. 5. FRAP image sequence for an elongated *E. coli* cell with TorA-GFP in the cytoplasm. The prebleach image is on the far left, and postbleach images have time in seconds indicated beneath them. The site of the bleach is indicated by the arrow, whose thickness corresponds to the approximate beam width. Scale bar, 5 microns.

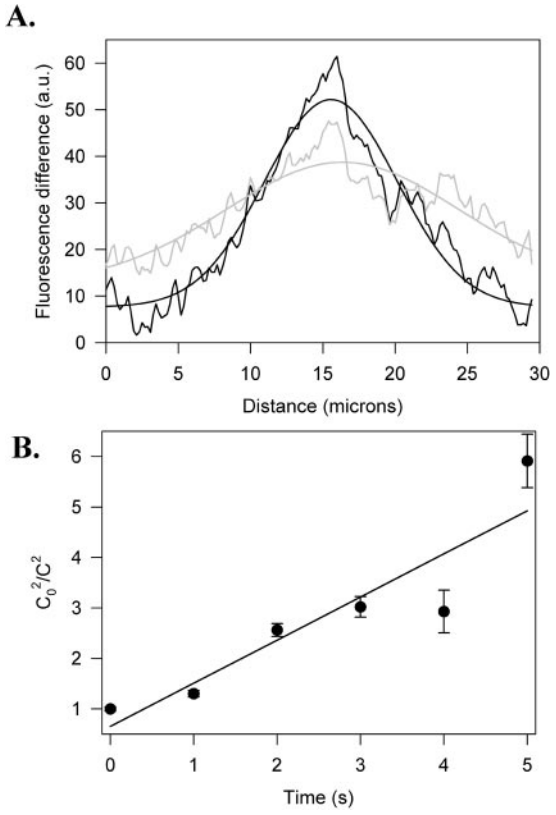

FIG. 6. Data analysis from a FRAP image sequence for an elongated *E. coli* cell with TorA-GFP in the cytoplasm. (A) One-dimensional fluorescence profiles from the first postbleach image (black) and 4 s later (gray). Raw data and fitted Gaussian curves are shown. The *x* axis shows distance along the long axis of the cell, and the *y* axis shows the fluorescence difference obtained by subtracting the postbleach fluorescence profiles from the prebleach profile. (B) Plot of C_0^2/C^2 versus time as described in the legend for Fig. 2.

proteolytic trimming of the N-terminal signal sequence (Fig. 4). However, this is unlikely to have a major effect on diffusion.

Because diffusion of TorA-GFP in the cytoplasm is rapid, FRAP measurements required a very brief bleaching period at high laser power levels, followed by the rapid acquisition of postbleach images. If the bleaching period was too prolonged, we found that TorA-GFP diffusion would spread the bleach over the entire cell during the bleaching period and before the acquisition of the first postbleach image. By increasing the laser power to the maximum possible, we were able to obtain a significant bleaching within about 0.5 s. Diffusion had already spread this bleach considerably before the acquisition of the first postbleach image, but in elongated cells, further spread and recovery of the bleach could be observed over the next few seconds (Fig. 5). As with TatA-GFP in the membrane, when fluorescence was bleached from an entire small cell aligned in the *x* direction, there was no detectable recovery on the time scale of the measurement (not shown). Thus, the fluorescence recovery we see arises from diffusion with no complications from delayed emission or other photochemical phenomena. Image sequences of the type shown in Fig. 5 provided sufficient information to allow an accurate diffusion coefficient to be calculated. Figure 6 shows an example of extracted one-dimensional fluorescence difference profiles for one cell and estimation of the diffusion coefficient from the time dependence of the depth of the bleach. With time, the bleach becomes shallower in the center and also spreads out, becoming broader. This is characteristic for diffusion (14). There was no indication of an immobile fraction of GFP, and the mean diffusion coefficient was $9.0 \pm 2.1\ \mu m^2\ s^{-1}$ ($n = 6$). This is very close to the previously reported value of $7.7 \pm 2.5\ \mu m^2\ s^{-1}$ for unmodified GFP diffusing in the *E. coli* cytoplasm (8).

Diffusion of TorA-GFP in the periplasm. As previously observed, we found that expression of TorA-GFP in the wild-type background led to the localization of GFP fluorescence in the periplasm (1, 23). We optimized the periplasmic location of TorA-GFP by inducing TorA-GFP expression with arabinose for 2 h, and then growing cells for a further 2 h in the absence of arabinose to allow time for as much of the TorA-GFP as possible to be exported (1). Cell fractionation and immunoblotting shows the overwhelmingly periplasmic location of GFP in cells grown in the presence of cephalexin under conditions identical to those used in the FRAP studies (Fig. 4). Only a minor fraction of GFP appears in the cytoplasm (Fig. 4). Fluorescence images showed GFP more clearly localized in the periplasms in some cells than in those of others (not shown). For FRAP measurements, we selected cells with the clearest periplasmic localization of GFP fluorescence. Thus, in the cells used for FRAP measurements, the periplasmic localization of GFP will be even more pronounced than that in the culture as a whole. Comparison of the high resolution fluorescence images in Fig. 3B and C shows the different distributions of TorA-GFP fluorescence in the wild-type and Δ*tatABCDE* backgrounds. Periplasmic GFP fluorescence levels were generally somewhat lower than those for cytoplasmic GFP. The *xy* resolution was about 0.25 μm so that fluorescence in the plasma membrane (Fig. 3A) and the periplasm (Fig. 3C) was visualized as a band of about 0.5 μm across, and the apparent diameter of the cell was increased from the true value of about 1 μm. Under these conditions, the optical *z* resolution of the confocal microscope was about 0.75 μm (half-width at half-maximum). This optical *z* resolution is not sufficient to give a

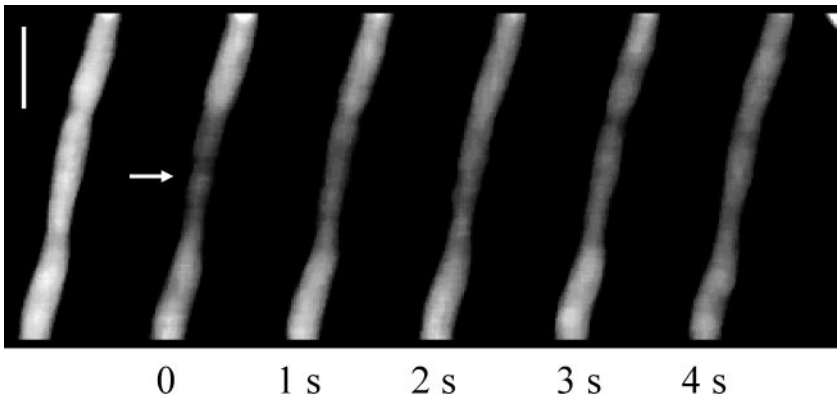

FIG. 7. FRAP image sequence for an elongated *E. coli* cell with TorA-GFP exported to the periplasm. The prebleach image is on the far left, and postbleach images have time in seconds indicated beneath them. The site of the bleach is indicated by the arrow, whose thickness corresponds to the approximate beam width. Scale bar, 5 microns.

clean optical section through the center of the cell. Some GFP fluorescence appears to come from the center of the cell in Fig. 3A and 3C, but in both cases, this is probably due mainly to out-of-focus fluorescence originating from GFP at the cell periphery. Cells were imaged at high resolution to confirm the periplasmic localization of GFP before carrying out FRAP measurements under the same conditions as for TorA-GFP in the cytoplasm.

A typical FRAP image sequence for periplasmic GFP is shown in Fig. 7. It is immediately apparent that, as for cytoplasmic GFP (Fig. 4), diffusion is rapid. As with GFP in the other cell environments, when fluorescence was bleached from an entire small cell aligned in the *x* direction, there was no detectable recovery on the time scale of the measurement (not shown). Thus, fluorescence recovery arises from diffusion with no complications from delayed emission or other photochemical phenomena. Figure 8 shows extracted one-dimensional fluorescence difference profiles and estimation of the diffusion coefficient from the time dependence of the depth of the bleach. Note that the bleach becomes shallower and broader with time, as is characteristic for diffusion (14). We observed a mean diffusion coefficient of $2.6 \pm 1.2\ \mu m^2\ s^{-1}$ ($n = 6$), about three times smaller than that for GFP diffusion in the cytoplasm. As with cytoplasmic GFP, there was no indication of an immobile fraction. A previous report indicated a protein diffusion coefficient in the *E. coli* periplasm about 300 times smaller than that which we observed (4). This raises the possibility that the rapid diffusion that we observed might be due to the movement of a small minority of GFP fluorescence in the cytoplasm. However, this idea is not consistent with our observations. If the level of GFP diffusion in the periplasm were substantially lower than that in the cytoplasm, we would expect the following. (i) The initial bleach in the periplasm would be very much more localized than that in the cytoplasm, because the periplasmic GFP would diffuse much less during the bleach and during the delay between the bleach and recording of the first image. (ii) Recovery of fluorescence in the periplasm would be very much smaller than that in the cytoplasm. (iii) Data analysis would reveal the presence of a substantial pool of GFP fluorescence that would appear immobile on short time scales.

Figure 3D through F presents a detailed comparison of fluorescence images before bleaching and at the beginning and end of a FRAP image sequence. The images recorded during the FRAP measurement (Fig. 3D through F) have low signal-to-noise ratios and low pixel resolutions due to the necessity of acquiring the

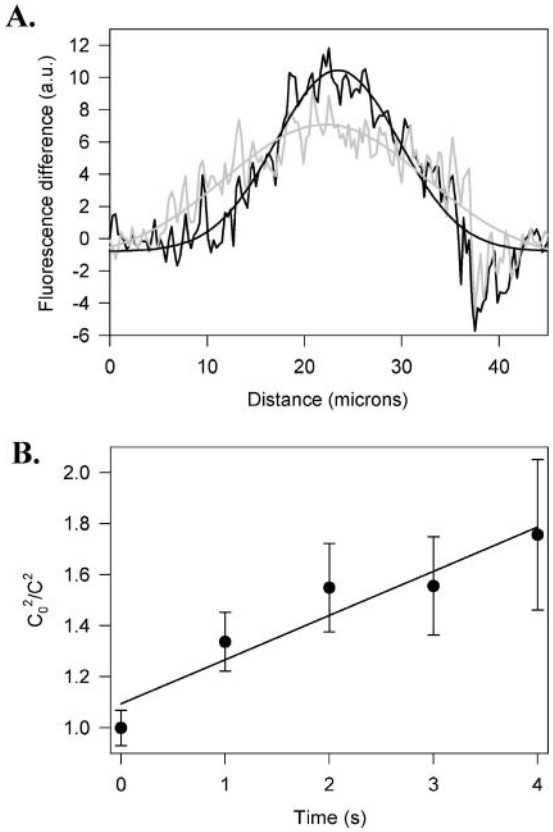

FIG. 8. Data analysis from a FRAP image sequence for an elongated *E. coli* cell with TorA-GFP exported to the periplasm. (A) One-dimensional fluorescence profiles from the first postbleach image (black) and 4 s later (gray). Raw data and fitted Gaussian curves are shown. The *x* axis shows distance along the long axis of the cell, and the *y* axis shows the fluorescence difference obtained by subtracting the postbleach fluorescence profiles from the prebleach profile. (B) Plot of C_0^2/C^2 versus time as described in the legend for Fig. 2.

images rapidly. Furthermore, they have low *z* resolution because, as for quantitative FRAP measurements, it is important that the measurement extends through the full depth of the cell (14, 15). Therefore, the FRAP images do not give a clear view of the periplasmic localization of GFP as seen in the high-resolution image of the same cell (Fig. 3C). Although the *z* resolution was decreased by opening the confocal pinhole, the *xy* resolution remained at about 250 nm and therefore was high enough to ensure that a significant shift in GFP fluorescence between the cytoplasm and the periplasm would result in the broadening or narrowing of the cell image. There is no indication that the initial bleach is more localized in the periplasm than that in the cytoplasm or that the rate of recovery of fluorescence is lower in the periplasm than that in the cytoplasm. The distribution of fluorescence in the cell at the end of the image sequence (after 10 s) (Fig. 3F) is similar to the distribution of fluorescence prior to the bleach (Fig. 3D), which confirms that there is no significant immobile fraction either in the periplasm or in the cytoplasm. We cannot exclude the possibility that the diffusion coefficient we measured is slightly skewed by the presence of a small proportion of rapidly diffusing GFP in the cytoplasm, but it is clear that the true diffusion coefficient for GFP in the periplasm cannot be substantially smaller than our measured value of $2.6 \pm 1.2\ \mu m^2\ s^{-1}$.

DISCUSSION

We have measured the lateral diffusion of GFP in three environments in *E. coli* cells: the cytoplasm, the periplasm, and the plasma membrane. In the cases of the cytoplasm and the periplasm, GFP was expressed with a short leader sequence which is cleaved upon export to the periplasm (1). As a heterologous protein, GFP is unlikely to have any specific interactions with other cell components, so to a first approximation, the GFP diffusion coefficient provides a measure of the physical environment in the cell: how fast can a water-soluble, 27-kDa globular protein diffuse? The true situation may not be quite so simple, however, since Elowitz et al. showed that the addition of a small histidine tag significantly lowers the diffusion rate of GFP in the cytoplasm and also that GFP diffusion rate becomes lower at high levels of GFP expression (8). We would expect native proteins generally to diffuse more slowly simply because they will be more liable to interact with other cell components. Nevertheless, it is important to have an understanding of how fast a protein can potentially diffuse in these environments.

Our measured lateral diffusion coefficient for GFP in the cytoplasm ($9.0 \pm 2.1\ \mu m^2\ s^{-1}$) is similar to that previously reported by Elowitz et al. using essentially the same experimental approach (8). Cluzel et al. (5) estimated the diffusion coefficient of a CheY-GFP fusion as $4.6 \pm 0.8\ \mu m^2\ s^{-1}$, by using fluorescence correlation spectroscopy. The slightly lower diffusion rate of CheY-GFP could be attributed to the larger size of the construct and possibly to specific interactions of CheY with other cell components.

In the periplasm, we measured a lateral diffusion coefficient for GFP of $2.6 \pm 1.2\ \mu m^2\ s^{-1}$, which is only about three times smaller than that in the cytoplasm. There has been a previous report of diffusion in the *E. coli* periplasm by Brass et al. (4). These authors added fluorescent tags to proteins in vitro. The labeled proteins were then introduced into periplasm by mixing them with *E. coli* cells permeabilized by calcium chloride treatment. The main protein used was maltose binding protein (MBP), a native component of the *E. coli* periplasm. However, for comparison, the authors also used other proteins, including cytochrome *c* and myoglobin, neither of which is native to *E. coli*. In all cases, the diffusion coefficients were remarkably small, being around 300 times smaller than our measured diffusion coefficient for GFP. In the case of MBP, the discrepancy could perhaps be explained by the native interactions of this protein with other components of the periplasm. However, this cannot apply to cytochrome *c* and myoglobin. We suggest several possible explanations. (i) The environment of the periplasm may be strongly and irreversibly perturbed by the calcium chloride treatment. Brass et al. commented that fluorescence was very variable from cell to cell (4). Even if the culture as a whole remained viable after calcium chloride treatment, those cells that were sufficiently fluorescent to be used for measurements were likely to have been particularly perturbed by the treatment. (ii) The loading of exogenous proteins into the periplasm may succeed only where those proteins already have, possibly just by chance, a strong affinity with other components of the periplasm. Thus, any protein that can be introduced into the periplasm by these means may show a rather low diffusion rate. (iii) The proteins may in fact have been adhering to the outer surface of the cell rather than being located in the periplasm. Controls performed by Brass et al. indicated that this was not the case with MBP, but it is possible that the other, heterologous proteins may not have been in the periplasm at all (4). (iv) Very rapid diffusion in a cell of limited size is technically difficult to measure. The FRAP procedure used by Brass et al. did not involve imaging cells during the FRAP measurement (4). Calculation of the diffusion coefficient depends on an estimate of the initial width of the bleach. In our experiments, this was measured from the first postbleach image in the FRAP sequence. Diffusion had already greatly broadened the bleach by the time the first image was recorded (Fig. 5). Brass et al. did not image the cells after bleaching and estimated the width of the bleach from the radius of the focused laser beam (4). If diffusion is rapid enough to be significant during the bleaching time (up to a few hundred milliseconds), then the initial bleach will in fact be much broader than this, leading to a considerable underestimate of the diffusion coefficient.

A subsequent report by the same group mentions rather higher estimates for the diffusion coefficients of galactose binding protein and maltose binding protein in the *E. coli* periplasm, although diffusion coefficients are not the main point of that paper and experimental details of the determination of diffusion coefficient are not given (9). The diffusion coefficients are still an order of magnitude below those that we observed. We cannot be sure of the explanation for the discrepancy, but we think that expression of GFP and export to the periplasm in vivo provides a much more reliable basis for probing the physical environment of the periplasm. We conclude that the periplasm is a relatively fluid environment, comparable to the cytoplasm in terms of its physical properties. This has important implications for understanding the dynamic processes that occur in the periplasm or on the periplasmic surface of the plasma membrane, including nutrient uptake, signaling, and electron transport. There is evidence for membrane adhesion

sites that join the plasma and outer membranes in gram-negative bacteria and are involved, for example, in the efflux of drugs (25). Such structures would be expected to act as diffusion barriers in the periplasm. However, we could detect no obvious diffusion barriers in our elongated *E. coli* cells. This confirms previous observations that there are no barriers to diffusion in the periplasm of cephalexin-treated *E. coli* cells (4, 9), although barriers to diffusion are present at predivision sites in filamented *fts*A mutant cells (9). In our cells, adhesion sites (if present) clearly do not extend around the full circumference of the cell or they provide only very transient barriers to diffusion. However, the presence of adhesion sites and other structures spanning the periplasm may well lower the diffusion rate of GFP and contribute to the effective viscosity of this cell compartment.

The effective viscosity (η_{eff}) of the cytoplasm and periplasm may be calculated from the ratio of the diffusion coefficient of GFP in water to the diffusion coefficient of GFP in the cell (18). The diffusion coefficient of GFP in water is 87 ± 2 μm^2 s^{-1} (18). Thus, we estimate η_{eff} to be 9.7 ± 2.3 cP in the *E. coli* cytoplasm and 34 ± 15 cP in the periplasm. For comparison with a eukaryotic cell, η_{eff} in the *Dictyostelium* cytoplasm is about 3.6 cP, with a significant contribution from the actin cytoskeletal network (18). Thus, the effective viscosity of the bacterial cytoplasm appears significantly higher. Protein concentrations are generally comparable in prokaryotic and eukaryotic cytoplasms (7), but the presence of the nucleoid in the prokaryotic cytoplasm is likely to significantly increase the effective viscosity.

We also report a diffusion coefficient of 0.13 ± 0.03 μm^2 s^{-1} for GFP fused to a native *E. coli* plasma membrane protein, TatA. To our knowledge, this is the first reported measurement of the lateral diffusion coefficient for a bacterial plasma membrane protein in vivo. In this case, GFP diffusion does not serve as a simple probe of the physical environment of the cell since TatA forms complexes with itself and with the other Tat proteins (3) which will inevitably strongly influence the diffusion coefficient. Thus, we cannot estimate the effective viscosity of the membrane. Bacterial plasma membranes differ from eukaryotic plasma membranes in several respects. They have different characteristic lipid compositions (16). In eukaryotes, the diffusion of membrane components is strongly influenced by interactions with the cortical cytoskeleton (16, 26). The prokaryotic cytoskeleton is more extensive than what was once thought but is somewhat different (13). It is also plausible that immobile components embedded in the cell wall could play a similar role in restricting plasma membrane protein diffusion. In spite of these differences, the diffusion coefficient for TatA-GFP is similar to that of a typical eukaryotic plasma membrane protein (26).

Diffusion studies on other *E. coli* plasma membrane proteins will provide crucial information on processes, including signal perception and electron transport. One particularly interesting dynamic system in *E. coli* is the *min* system, which locates the site of septum formation at the midpoint of the cell (12). Dynamic modeling of the *min* system is based on the assumption that protein diffusion in the cytoplasm is much more rapid than that in the plasma membrane (12), an assumption that is borne out by our findings.

ACKNOWLEDGMENTS

This work was supported by grants from the Wellcome Trust to C.W.M. and the Biotechnology and Biological Sciences Research Council to C.R.

REFERENCES

1. **Barrett, C. M. L., N. Ray, J. D. Thomas, C. Robinson, and A. Bolhuis.** 2003. Quantitative export of a reporter protein, GFP, by the twin-arginine translocation pathway in *Escherichia coli*. Biochem. Biophys. Res. Commun. **304:** 279–284.
2. **Bolhuis, A., E. G. Bogsch, and C. Robinson.** 2000. Subunit interactions in the twin-arginine translocase complex of *Escherichia coli*. FEBS Lett. **472:**88–92.
3. **Bolhuis, A., J. E. Mathers, J. D. Thomas, C. Barrett, and C. Robinson.** 2001. TatB and TatC form a functional and structural unit of the twin-arginine translocase from *Escherichia coli*. J. Biol. Chem. **276:**20213–20219.
4. **Brass, J. M., C. F. Higgins, M. Foley, P. A. Rugman, J. Birmingham, and P. B. Garland.** 1986. Lateral diffusion of proteins in the periplasm of *Escherichia coli*. J. Bacteriol. **165:**787–795.
5. **Cluzel, P., M. Surette, and S. Leibler.** 2000. An ultrasensitive bacterial motor revealed by monitoring signaling proteins in single cells. Science **287:**1652–1654.
6. **Cormack, B. P., R. H. Valdivia, and S. Falkow.** 1996. FACS-optimized mutants of the green fluorescent protein (GFP). Gene **173:**33–38.
7. **Ellis, R. J.** 2001. Macromolecular crowding: an important but neglected aspect of the intracellular environment. Curr. Opin. Struct. Biol. **11:**114–119.
8. **Elowitz, M. B., M. G. Surette, P.-E. Wolf, J. B. Stock, and S. Leibler.** 1999. Protein mobility in the cytoplasm of *Escherichia coli*. J. Bacteriol. **181:**197–203.
9. **Foley, M., J. M. Brass, J. Birmingham, W. R. Cook, P. B. Garland, C. F. Higgins, and L. I. Rothfield.** 1989. Compartmentalization of the periplasm at cell division sites in *Escherichia coli* as shown by fluorescence photobleaching experiments. Mol. Microbiol. **3:**1329–1336.
10. **Guzman, L.-M., D. Belin, M. J. Carson, and J. Beckwith.** 1995. Tight regulation, modulation, and high-level expression by vectors containing the arabinose P-BAD promoter. J. Bacteriol. **177:**4121–4130.
11. **Kubitscheck, U., P. Wedekind, and R. Peters.** 1994. Lateral diffusion measurement at high spatial resolution by scanning microphotolysis in a confocal microscope. Biophys. J. **67:**948–956.
12. **Lutkenhaus, J.** 2002. Dynamic proteins in bacteria. Curr. Opin. Microbiol. **5:**548–552.
13. **Møller-Jensen, J., and J. Löwe.** 2005. Increasing complexity of the bacterial cytoskeleton. Curr. Opin. Cell Biol. **17:**75–81.
14. **Mullineaux, C. W., M. J. Tobin, and G. R. Jones.** 1997. Mobility of photosynthetic complexes in thylakoid membranes. Nature **390:**421–424.
15. **Mullineaux, C. W., and M. Sarcina.** 2002. Probing the dynamics of photosynthetic membranes with fluorescence recovery after photobleaching. Trends Plant Sci. **7:**237–240.
16. **Opekarova, M., and W. Tanner.** 2003. Specific lipid requirements of membrane proteins—a putative bottleneck in heterologous expression. Biochim. Biophys. Acta **1610:**11–22.
17. **O'Toole, P. J., C. Wolfe, S. Ladha, and R. J. Cherry.** 1999. Rapid diffusion of spectrin bound to a lipid surface. Biochim. Biophys. Acta. **1419:**64–70.
18. **Potma, E. O., W. P. de Boeij, L. Bosgraaf, J. Roelofs, P. J. M. van Haastert, and D. A. Wiersma.** 2001. Reduced protein diffusion rate by cytoskeleton in vegetative and polarized *Dictyostelium* cells. Biophys. J. **81:**2010–2019.
19. **Ray, N., A. Nenninger, C. W. Mullineaux, and C. Robinson.** 2005. Location and mobility of twin-arginine translocase subunits in the *Escherichia coli* plasma membrane. J. Biol. Chem. **280:**17961–17968.
20. **Reits, E. A. J., and J. J. Neefjes.** 2001. From fixed to FRAP: measuring protein mobility and activity in living cells. Nature Cell Biol. **3:**145–147.
21. **Sarcina, M., M. J. Tobin, and C. W. Mullineaux.** 2001. Diffusion of phycobilisomes on the thylakoid membranes of the cyanobacterium *Synechococcus* 7942: effects of phycobilisome size, temperature and membrane lipid composition. J. Biol. Chem. **276:**46830–46834.
22. **Sarcina, M., N. Murata, M. J. Tobin, and C. W. Mullineaux.** 2003. Lipid diffusion in the thylakoid membranes of the cyanobacterium *Synechococcus* sp.: effect of fatty acid desaturation. FEBS Lett. **553:**295–298.
23. **Thomas, J. D., R. A. Daniel, J. Errington, and C. Robinson.** 2001. Export of active green fluorescent protein to the periplasm by the twin-arginine translocase (Tat) pathway in *Escherichia coli*. Mol. Microbiol. **39:**47–53.
24. **Wexler, M., F. Sargent, R. L. Jack, N. R. Stanley, E. G. Bogsch, C. Robinson, B. C. Berks, and T. Palmer.** 2000. TatD is a cytoplasmic protein with DNase activity—no requirement for TatD family proteins in Sec-independent protein export. J. Biol. Chem. **275:**16717–16722.
25. **Zgurskaya, H. I., and H. Nikaido.** 2000. Multidrug resistance mechanisms: drug efflux across two membranes. Mol. Microbiol. **37:**219–225.
26. **Zhang, F., G. M. Lee, and K. Jacobson.** 1993. Protein lateral mobility as a reflection of membrane microstructure. Bioessays **15:**579–588.